Multistage Melt Polymerization of Bisphenol-A and Diphenyl Carbonate to Polycarbonate

YANGSOO KIM and KYU YONG CHOI*

Department of Chemical Engineering, University of Maryland, College Park, Maryland 20742

SYNOPSIS

A multistage melt polycondensation of bisphenol-A and diphenyl carbonate has been studied experimentally using $LiOH \cdot H_2O$ catalyst. The reaction process consists of batch and semibatch periods with different temperature and pressure conditions. It was observed that a small amount of diphenyl carbonate lost from the reaction mixture by vaporization had little effect on the molecular weight in the batch reaction period but the efficiency of subsequent low-pressure semibatch polycondensation was affected by the change in the mol ratio of the phenyl carbonate group to the hydroxyl end group. A molecular species model developed for the multistage process was used to analyze the kinetics of the polycondensation process. The composition of the reaction mixture was analyzed by HPLC and compared with model simulations. In particular, the effect of evaporative loss of diphenyl carbonate on the progress of reaction is discussed in detail. © 1993 John Wiley & Sons, Inc.

INTRODUCTION

Polycarbonate is an important engineering thermoplastic having many useful properties. Currently, polycarbonate is produced on a commercial scale by an interfacial phosgenation process in which bisphenol-A (4,4-dihydroxydiphenyl 2,2-propane; BPA) salt in an aqueous caustic solution is reacted with phosgene in an organic solution. The bisphenol-A polycarbonate can also be prepared by melt transesterification of diphenyl carbonate (DPC) with bisphenol-A. The melt transesterification process has some advantages over the interfacial phosgenation process in that no toxic solvents are used and that final polymers can be directly pelletized. However, the melt transesterification process also poses some problems. For example, specially designed reactor equipment is required to deal with highly viscous polymer melt to obtain high molecular weight polymers under high temperature and vacuum conditions. The employment of high reaction temperature (280–300°C) may also cause unwanted side reactions, leading to discoloration, branching, and crosslinking.

The transesterification of DPC and BPA is a reversible reaction and the reaction byproduct (phenol) should be distilled off continuously to facilitate the forward chain growth reaction. Phenol is removed from the liquid phase by applying high vacuum; however, its removal rate decreases significantly as the melt viscosity increases with the formation of high molecular weight polymers. Since DPC exhibits moderate vapor pressure at 250–300°C, some DPC may be lost from the reactor during the initial reaction stage unless reaction temperature and pressure are properly controlled. Any loss of DPC during the reaction will cause significant variations in the concentration of reactive end groups (phenyl carbonate and hydroxyl groups) that, in turn, will make high molecular weight polymers difficult to obtain. Therefore, it is desirable to minimize the loss of DPC by operating the reactor in multistages using different reaction conditions in each stage. For example, the transesterification may be carried out first in a batch mode until monomers are converted to less volatile oligomers. Then, the reactor can be operated in a semibatch mode at reduced pressure and increased temperature. Quite obviously, understanding the transesterification kinetics and associated mass transfer phenomena will play an important role in designing optimal multistage polymerization strategies.

* To whom correspondence should be addressed.

Journal of Applied Polymer Science, Vol. 49, 747–764 (1993)
 CCC 0021-8995/93/050747-18

Unfortunately, there is a dearth of open literature on the kinetics of melt polycarbonate synthesis processes. Losev et al.[1] investigated the transesterification of DPC with BPA using zinc oxide (ZnO) as a catalyst. They carried out the reaction in two successive stages (stage 1: 200–210°C, 50–70 mmHg, 2–3 h; stage 2: gradual increase of temperature from 230 to 280°C, ~ 1 mmHg, completion of reaction in 5–6 h) with 10 reaction tubes placed in a constant temperature bath. They assumed that the condensates liberated from the reaction tubes were pure phenol, yet the reported amount of phenol evolved was greater than the theoretical amount of phenol to be produced at the complete conversion of reaction, suggesting that some entrainment of reactants might have occurred. In our recent experimental study,[2] it was observed that when the vacuum was applied in the beginning of the reaction, even at a temperature lower than 200°C, the condensate contained not only phenol but also small amounts of diphenyl carbonate and bisphenol-A. Turska and Wróbel[3,4] studied the kinetics of the melt transesterification of DPC with BPA using zinc oxide (ZnO) as a catalyst at 200–250°C and 60 mmHg. Recently, Hersh and Choi[5] and Kim et al.[6] reported a batch experimental study of melt transesterification of DPC and BPA using lithium hydroxide monohydrate ($LiOH \cdot H_2O$) as a catalyst. They analyzed the reaction products withdrawn from the reactor during the reaction and reported forward and reverse reaction rate constants for both catalyzed and uncatalyzed transesterifications.

In this paper, we shall report an experimental and modeling study of a multistage transesterification process using a mechanically agitated reactor. The effects of evaporative loss of DPC on the progress of reaction and resulting polymer properties (i.e., polymer molecular weights and functional end group distribution) will be presented.

EXPERIMENTAL

A schematic diagram of a bench scale semibatch melt transesterification reactor is shown in Figure 1. In performing semibatch transesterification experiments, it is important to distill off phenol and to reflux DPC to the reactor so that initial mol ratio of phenyl carbonate group to hydroxyl group is maintained during the reaction. To distill off phenol, a jacketed glass distillation column and a condenser are installed in the vacuum line between the reactor and a cold trap. The distillation column temperature is maintained at the temperature above the boiling

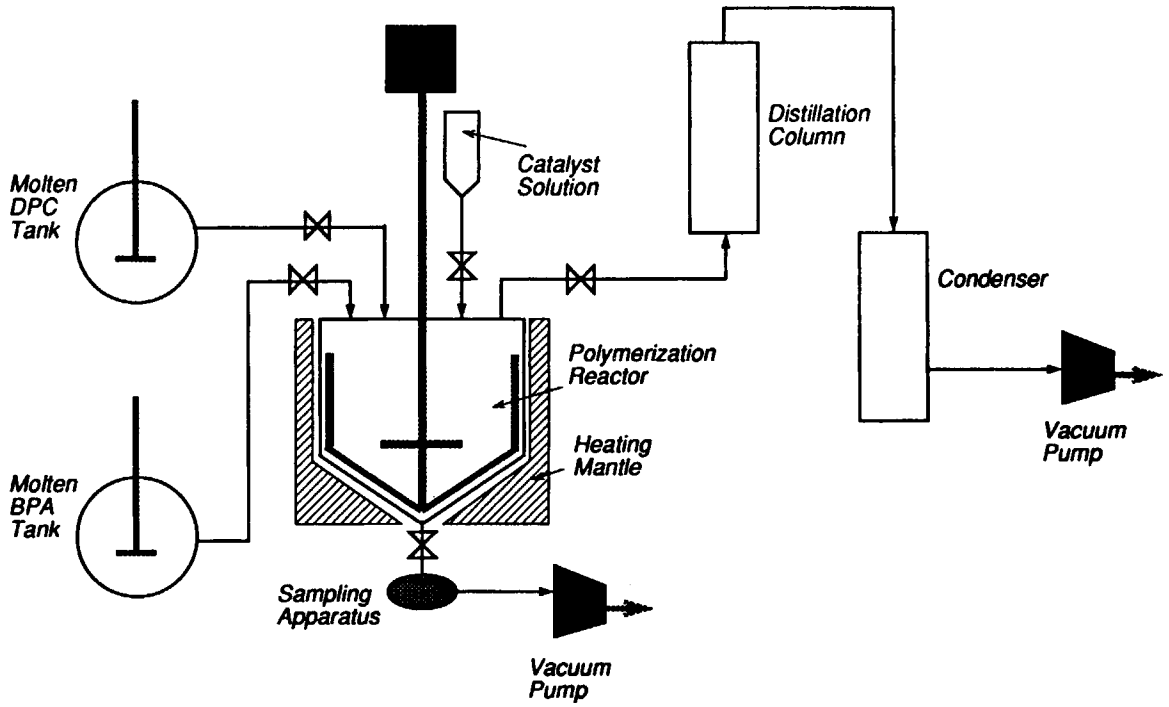

Figure 1 Experimental semibatch reactor system.

Table I Experimental Reaction Conditions

	Run-I			Run-II		
	$(BPA)_0$ = 1.15 mol $(DPC/BPA)_0$ = 1.22 [LiOH] = 3.65×10^{-5} mol/mol $(BPA)_0$			$(BPA)_0$ = 1.31 mol $(DPC/BPA)_0$ = 1.07 [LiOH] = 3.21×10^{-5} mol/mol $(BPA)_0$		
Stage No.	Time (min)	Temp (°C)	Pressure (mmHg)	Time (min)	Temp (°C)	Pressure (mmHg)
Batch						
1	0–120	180	1480	0–120	230	1480
2	120–153	180 → 250	1480	120–142	230 → 250	1480
Semibatch						
3	153–273	250	150 (1 h) 50 (1 h)	142–262	250	150 (1 h) 50 (1 h)
4	273–298	250 → 280	50	262–297	250 → 280	50
5	298–358	280	10	297–357	280	10

point of phenol but below the boiling point of DPC for a given reactor pressure (e.g., 150°C at 50 mmHg).

The reactor operating conditions for the two reaction experiments are summarized in Table I. The DPC and BPA melting tanks are first charged with a predetermined amount of DPC (Aldrich) and BPA (*Parabis* resin from Dow Chemical Co.). Since the reaction starts almost immediately after BPA and DPC are mixed even without catalyst, BPA and DPC melts are supplied separately into the reactor. High-purity BPA was used as supplied and DPC was recrystallized from 2-propanol and vacuum-dried for more than 10 h. It was observed that the actual molar ratio of DPC to BPA in the reactor after these monomers were discharged to the reactor differed slightly from the ratio before the discharge, due to small amounts of BPA being left in the feed lines after the molten BPA was discharged from the storage tank.

The initial DPC/BPA molar ratio in the reactor was determined by HPLC after taking a small amount of sample from the reactor prior to the injection of catalyst. The catalyst ($LiOH \cdot H_2O$) was dissolved in deionized water and injected into the reactor through a separate injection port. The starting reaction time was defined as the moment when the catalyst was injected into the reactor after the reactor reached a desired temperature. The initial composition of the reactant mixture determined by HPLC was used as the initial condition for corresponding model simulations. As shown in Table I, the reaction was carried out in five stages: In the first stage, the reaction was conducted in a batch mode under nitrogen atmosphere. The purpose of operating the reactor in the batch mode prior to semibatch operation is to convert as much DPC as possible to low molecular weight oligomers so that a minimum amount of free DPC is present in subsequent semibatch operations. A major difference between the two experimental runs was that the starting temperatures were different. In each run, the batch reactor temperature was gradually raised to 250°C (stage 2) before the reactor pressure was reduced. At the beginning of third stage, reactor pressure was at first reduced to 760 mmHg and then further reduced to 150 mmHg and the reaction was continued at 250°C for 1 h. At this temperature, the reactor was operated at 50 mmHg for 1 more hour. In stage 4, the reactor temperature was raised from 250 to 280°C at 50 mmHg. In stage 5, the reactor pressure was lowered to 10 mmHg and the reaction was continued for 1 h at 280°C. This procedure is very similar to one of the examples described in the patent literature.[7]

Small amounts of reaction samples were withdrawn from the reactor at different reaction times by attaching a small sampling flask (25 mL) to the bottom of the reactor and then opening the sampling valve. The sampling flask was connected to a vacuum pump. The sampling did not disturb the reactor pressure because the sampling was done almost instantaneously and the amount of sample was very small. Although there were no difficulties in sampling the reaction products until stage 4 (i.e., 250°C and 50 mmHg), the sampling became difficult af-

terward because the melt viscosity was too high. Thus, no samples were taken in stage 5 and only the final product was analyzed. The composition of the reaction mixture was determined by HPLC using the method reported by Bailly et al.[8] The composition of the liquid condensates was also measured by HPLC with a C-18 column using an acetonitrile–water mixture (40/60, v/v) as a solvent and 4-*tert*-butyl phenol as an internal standard. The polymer molecular weight excluding unreacted monomers present in the reaction mixture was determined by HPLC for the reaction samples taken during the batch period and by size exclusion chromatography (SEC) for those taken during the semibatch period.

REACTION MODEL

For the modeling of batch and semibatch melt transesterification reactors, one can use either a functional group model or a molecular species model. With the functional group model, the overall conversion of reactive end groups in various molecules including monomers can be easily calculated. In the reaction system where some monomers (e.g., DPC) evaporate during the reaction, the molecular species modeling approach is more convenient to calculate the variations in the monomer concentrations and the molecular weight of oligomers and polymers excluding monomers. Therefore, we shall develop a molecular species model for our reaction system. The melt transesterification of DPC and BPA is represented by the following sequence of reactions:

$$A_n + B_m \rightleftharpoons C_{n+m+1} + P \quad (n, m \geq 0) \tag{1}$$

$$B_n + C_m \rightleftharpoons B_{n+m} + P \quad (n \geq 0, m \geq 1) \tag{2}$$

$$A_n + C_m \rightleftharpoons A_{n+m} + P \quad (n \geq 0, m \geq 1) \tag{3}$$

$$C_n + C_m \rightleftharpoons C_{n+m} + P \quad (n, m \geq 1) \tag{4}$$

where P is phenol and the three polymeric species (A_n, B_n, and C_n) are defined as follows:

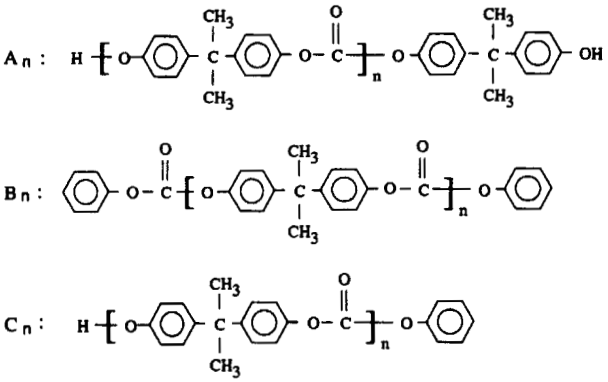

Note that A_0 is bisphenol-A; B_0, diphenol carbonate, and C_1, the monophenyl carbonate of BPA.

Assuming that the reactivities of the functional end groups are independent of the chain length, we can derive the following component molar mass balance equations:

$$\frac{dA_0}{dt} = \frac{1}{V}\left[-2kA_0\left\{2B_0 + \sum_{n=1}^{\infty}(2B_n + C_n)\right\} + k'P\sum_{n=1}^{\infty}(2A_n + C_n)\right] \tag{5}$$

$$\frac{dB_0}{dt} = \frac{1}{V}\left[-2kB_0\left\{2A_0 + \sum_{n=1}^{\infty}(2A_n + C_n)\right\} + k'P\sum_{n=1}^{\infty}(2B_n + C_n)\right] \tag{6}$$

$$\frac{dP}{dt} = \frac{1}{V}\left[k\left[4\left(A_0 + \sum_{n=1}^{\infty}A_n\right)\left(B_0 + \sum_{n=1}^{\infty}B_n\right) + 2\sum_{n=1}^{\infty}C_n\left\{\left(A_0 + \sum_{m=1}^{\infty}A_m\right) + \left(B_0 + \sum_{m=1}^{\infty}B_m\right)\right\}\right.\right.$$
$$\left.\left. + \left(\sum_{n=1}^{\infty}C_n\right)^2\right] - k'P\left\{\sum_{n=1}^{\infty}(2nA_n + 2nB_n + nC_n) + \sum_{n=2}^{\infty}(n-1)C_n\right\}\right] \tag{7}$$

$$\frac{dA_n}{dt} = \frac{1}{V}\left[2k\left\{-2A_nB_0 - A_n\sum_{m=1}^{\infty}(2B_m + C_m) + \sum_{r=1}^{n}A_{n-r}C_r\right\}\right.$$
$$\left. + k'P\left\{\sum_{r=n+1}^{\infty}(C_r + 2A_r) - 2nA_n\right\}\right] \quad (n \geq 1) \tag{8}$$

$$\frac{dB_n}{dt} = \frac{1}{V}\left[2k\left\{-2B_nA_0 - B_n\sum_{m=1}^{\infty}(2A_m + C_m) + \sum_{r=1}^{n}B_{n-r}C_r\right\} + k'P\left\{\sum_{r=n+1}^{\infty}(C_r + 2B_r) - 2nB_n\right\}\right] \quad (n \geq 1) \quad (9)$$

$$\frac{dC_n}{dt} = \frac{1}{V}\left[2k\left\{2\sum_{r=0}^{n-1}A_{n-r-1}B_r - (A_0 + B_0)C_n - C_n\sum_{m=1}^{\infty}(A_m + B_m + C_m) + \frac{1}{2}\sum_{r=1}^{n-1}C_rC_{n-r}\right\} + k'P\left\{-(2n-1)C_n + 2\sum_{r=n}^{\infty}(A_r + B_r) + 2\sum_{r=n+1}^{\infty}C_r\right\}\right] \quad (n \geq 1) \quad (10)$$

In the above model equations, the capital letters represent the number of moles of that particular component, and V, the reaction volume.

For the calculation of molecular weight averages, the following moment equations are also derived and solved:

$$V\frac{dA_0}{dt} = k[-4A_0B_0 - 4A_0\lambda_{B,0} - 2A_0\lambda_{C,0}] + k'[P\lambda_{C,0} + 2P\lambda_{A,0}] \quad (11)$$

$$V\frac{dB_0}{dt} = k[-4A_0B_0 - 4B_0\lambda_{A,0} - 2B_0\lambda_{C,0}] + k'[P\lambda_{C,0} + 2P\lambda_{B,0}] \quad (12)$$

$$V\frac{dP}{dt} = k[4A_0B_0 + 4A_0\lambda_{B,0} + 4B_0\lambda_{A,0} + 4\lambda_{A,0}\lambda_{B,0} + 2A_0\lambda_{C,0} + 2\lambda_{A,0}\lambda_{C,0} + 2B_0\lambda_{C,0} + 2\lambda_{B,0}\lambda_{C,0} + (\lambda_{C,0})^2] + k'[-2P\lambda_{C,1} - 2P\lambda_{A,1} - 2P\lambda_{B,1} + P\lambda_{C,0}] \quad (13)$$

$$V\frac{d\lambda_{A,0}}{dt} = k[-4B_0\lambda_{A,0} - 4\lambda_{A,0}\lambda_{B,0} + 2A_0\lambda_{C,0}] + k'[P\lambda_{C,1} - P\lambda_{C,0} - 2P\lambda_{A,0}] \quad (14)$$

$$V\frac{d\lambda_{A,1}}{dt} = k[-4B_0\lambda_{A,1} - 4\lambda_{A,1}\lambda_{B,0} + 2A_0\lambda_{C,1} + 2\lambda_{A,0}\lambda_{C,1}] + k'\left[\frac{1}{2}P\lambda_{C,2} - \frac{1}{2}P\lambda_{C,1} - P\lambda_{A,2} - P\lambda_{A,1}\right] \quad (15)$$

$$V\frac{d\lambda_{A,2}}{dt} = k[-4B_0\lambda_{A,2} - 4\lambda_{A,2}\lambda_{B,0} + 2A_0\lambda_{C,2} + 4\lambda_{A,1}\lambda_{C,1} + 2\lambda_{A,0}\lambda_{C,2}] + k'\left[\frac{1}{3}P\lambda_{C,3} - \frac{1}{2}P\lambda_{C,2} + \frac{1}{6}P\lambda_{C,1} - \frac{4}{3}P\lambda_{A,3} - P\lambda_{A,2} + \frac{1}{3}P\lambda_{A,1}\right] \quad (16)$$

$$V\frac{d\lambda_{B,0}}{dt} = k[-4A_0\lambda_{B,0} - 4\lambda_{A,0}\lambda_{B,0} + 2B_0\lambda_{C,0}] + k'[P\lambda_{C,1} - P\lambda_{C,0} - 2P\lambda_{B,0}] \quad (17)$$

$$V\frac{d\lambda_{B,1}}{dt} = k[-4A_0\lambda_{B,1} - 4\lambda_{B,1}\lambda_{A,0} + 2B_0\lambda_{C,1} + 2\lambda_{B,0}\lambda_{C,1}] + k'\left[\frac{1}{2}P\lambda_{C,2} - \frac{1}{2}P\lambda_{C,1} - P\lambda_{B,2} - P\lambda_{B,1}\right] \quad (18)$$

$$V\frac{d\lambda_{B,2}}{dt} = k[-4A_0\lambda_{B,2} - 4\lambda_{B,2}\lambda_{A,0} + 2B_0\lambda_{C,2} + 4\lambda_{B,1}\lambda_{C,1} + 2\lambda_{B,0}\lambda_{C,2}] + k'\left[\frac{1}{3}P\lambda_{C,3} - \frac{1}{2}P\lambda_{C,2} + \frac{1}{6}P\lambda_{C,1} - \frac{4}{3}P\lambda_{B,3} - P\lambda_{B,2} + \frac{1}{3}P\lambda_{B,1}\right] \quad (19)$$

$$V\frac{d\lambda_{C,0}}{dt} = k[4A_0B_0 + 4A_0\lambda_{B,0} + 4\lambda_{A,0}B_0 + 4\lambda_{A,0}\lambda_{B,0} - 2A_0\lambda_{C,0} - 2\lambda_{A,0}\lambda_{C,0} - 2B_0\lambda_{C,0} - 2\lambda_{B,0}\lambda_{C,0} - (\lambda_{C,0})^2] + k'[-P\lambda_{C,0} + 2P\lambda_{A,1} + 2P\lambda_{B,1}] \quad (20)$$

$$V\frac{d\lambda_{C,1}}{dt} = k[4A_0B_0 + 4A_0\lambda_{B,1} + 4A_0\lambda_{B,0} + 4B_0\lambda_{A,0} + 4B_0\lambda_{A,1} + 4\lambda_{A,1}\lambda_{B,0} + 4\lambda_{A,0}\lambda_{B,1} + 4\lambda_{A,0}\lambda_{B,0} - 2A_0\lambda_{C,1} - 2\lambda_{A,0}\lambda_{C,1} - 2B_0\lambda_{C,1} - 2\lambda_{B,0}\lambda_{C,1}] + k'[P\lambda_{B,1} - P\lambda_{C,2} + P\lambda_{A,1} + P\lambda_{B,2} + P\lambda_{A,2}] \quad (21)$$

$$V\frac{d\lambda_{C,2}}{dt} = k[4A_0B_0 + 4A_0\lambda_{B,2} + 8A_0\lambda_{B,1} + 4A_0\lambda_{B,0} + 4\lambda_{A,2}B_0 + 4\lambda_{A,2}\lambda_{B,0} + 8\lambda_{A,1}B_0 + 8\lambda_{A,1}\lambda_{B,1} + 8\lambda_{A,1}\lambda_{B,0} + 4\lambda_{A,0}B_0 + 4\lambda_{A,0}\lambda_{B,2} + 8\lambda_{A,0}\lambda_{B,1} + 4\lambda_{A,0}\lambda_{B,0} - 2A_0\lambda_{C,2} - 2\lambda_{A,0}\lambda_{C,2} - 2B_0\lambda_{C,2} - 2\lambda_{B,0}\lambda_{C,2} + 2(\lambda_{C,1})^2] + k'\left[\frac{2}{3}P\lambda_{A,3} + P\lambda_{A,2} + \frac{1}{3}P\lambda_{A,1} + \frac{2}{3}P\lambda_{B,3} + P\lambda_{B,2} + \frac{1}{3}P\lambda_{B,1} - \frac{4}{3}P\lambda_{C,3} + \frac{1}{3}P\lambda_{C,1}\right] \quad (22)$$

In the above, the k-th molecular weight moments for A_n, B_n, and C_n-type polymeric species are defined as

$$\lambda_{A,k} = \sum_{n=1}^{\infty} n^k A_n \quad \lambda_{B,k} = \sum_{n=1}^{\infty} n^k B_n \quad \lambda_{C,k} = \sum_{n=1}^{\infty} n^k C_n \quad (23)$$

The third moment, which is dependent on the second moment, is calculated using the following moment closure formula:[9]

$$\lambda_{i,3} = \frac{\lambda_{i,2}(2\lambda_{i,2}\lambda_{i,0} - \lambda_{i,1}^2)}{\lambda_{i,1}\lambda_{i,0}} \quad (i = A, B, C) \quad (24)$$

Then, the number-average molecular weight ($\overline{M_n}$) and the weight-average molecular weight ($\overline{M_w}$) are calculated as follows:

$$\overline{M_n} = \frac{\sum_{n=1}^{\infty}(A_nW_{A_n} + B_nW_{B_n} + C_nW_{C_n})}{\sum_{n=1}^{\infty}(A_n + B_n + C_n)} = \frac{S_1}{S_0} \quad (25)$$

$$\overline{M_w} = \frac{\sum_{n=1}^{\infty}(A_nW_{A_n}^2 + B_nW_{B_n}^2 + C_nW_{C_n}^2)}{\sum_{n=1}^{\infty}(A_nW_{A_n} + B_nW_{B_n} + C_nW_{C_n})} = \frac{S_2}{S_1} \quad (26)$$

where $S_0 = \lambda_{A,0} + \lambda_{B,0} + \lambda_{C,0}$; $S_1 = (254.3)(\lambda_{A,1} + \lambda_{B,1} + \lambda_{C,1}) + (228.29)\lambda_{A,0} + (214.22)\lambda_{B,0} + (94.11)\lambda_{C,0}$; and $S_2 = (254.3)^2(\lambda_{A,2} + \lambda_{B,2} + \lambda_{C,2}) + (2)(254.3)[(228.29)\lambda_{A,1} + (214.22)\lambda_{B,1} + (94.11)\lambda_{C,1}] + (228.29)^2\lambda_{A,0} + (214.22)^2\lambda_{B,0} + (94.11)^2\lambda_{C,0}$.

Here, the molecular weight of each polymeric species (A_n, B_n, C_n) is given by

$$W_{A_n} = (254.3)n + 228.29$$

$$W_{B_n} = (254.3)n + 214.22$$

$$W_{C_n} = (254.3)n + 94.11$$

Note in the above equations that the contribution of each end group to the molecular weight of each polymeric species has been accounted for. This end-group effect, although negligible in high molecular weight polymers, should be included in calculating the molecular weight of low molecular weight polymers.

The rate constants in the above model are the effective rate constants in which the catalyst concentration effect is incorporated, i.e., $k = \boldsymbol{k}(N^*/V)$, $k' = \boldsymbol{k}'(N^*/V)$, where N^* is the number of moles of catalyst added and V is the volume of reaction mixture. The numerical values of the rate constants are given in Table II. In semibatch operations, the effective catalyst concentration increases as the reaction proceeds because volatile components are removed from the reactor and the liquid-phase volume decreases accordingly. It is assumed that the catalyst does not deactivate during the reaction. The volume of the reaction mixture (V) is updated in each time step by subtracting the liquid-equivalent volumes of evaporated phenol and DPC from the reactor volume in the previous time step. The net amount of DPC removed from the reactor is the difference between the amount vaporized from the liquid phase and that refluxed to the reactor via a distillation column. Oligomers or polymers are assumed not to vaporize.

In semibatch operations, one needs to know how much phenol and monomers vaporize at given tem-

Table II Kinetic Parameters and Physical Constants

	Expression	Unit	Ref.
$\boldsymbol{k}$	$\boldsymbol{k} = 8.50 \times 10^7 \exp(-14{,}200/RT)$	$\frac{L^2}{mol^2 min}$	6
$\boldsymbol{k}'$	$\boldsymbol{k}' = 7.31 \times 10^6 \exp(-12{,}100/RT)$	$\frac{L^2}{mol^2 min}$	6
$\hat{v}_P$	8.79×10^{-2}	$\frac{L}{mol}$	
$\hat{v}_{B_0}$	1.68×10^{-1}	$\frac{L}{mol}$	
$\hat{v}_{A_0}$	1.91×10^{-1}	$\frac{L}{mol}$	
p_P^0	$\log p_P^0 = 7.13457 - \frac{1{,}516.072}{T - 98.581}$	mmHg	10
$p_{B_0}^0$	$\log p_{B_0}^0 = \left(-\frac{14.76 \times 10^3}{1.987}\right) \cdot \frac{1}{T} + 19.5521$	mmHg	
$p_{A_0}^0$	$\ln\left(\frac{p_{A_0}^0}{7.502}\right) = A + \frac{B}{T} + C \cdot T + D \cdot T^2$ $A = 45.015 \quad B = -1.590 \times 10^6$ $C = -3.764 \times 10^{-2} \quad D = 2.129 \times 10^{-5}$	mmHg	11

perature and pressure. In Table II, vapor pressure correlations for phenol, BPA, and DPC are listed. The correlation for DPC was constructed using two reported vapor-pressure data (i.e., at 302°C, 1 atm, and at 168°C, 15 mmHg).[12] We have also used a SWAP method proposed by Smith et al.[13] to calculate the vapor pressure of DPC. The vapor pressure predictions using the correlation shown in Table II and the SWAP method were almost identical.

As the reactor pressure is lowered after the batch stage is completed, volatiles are removed and the composition of the liquid phase changes. Assuming that the vapor phase follows the ideal gas law, we can represent the partial pressure of the volatile species j in the vapor phase as

$$p_j = p_t y_j = \gamma_j p_j^0 x_j \tag{27}$$

where y_j is the mol fraction of component j in the vapor phase; x_j, the mol fraction of j in the liquid phase; p_t, the total pressure; p_j^0, the saturated vapor pressure of component j; and γ_j, the activity coefficient of j. The activity coefficients of phenol (γ_P) and DPC (γ_{B_0}) are calculated using the Flory–Huggins equation[14]:

$$\ln \gamma_j = \ln[1 - (1 - 1/m_j)(1 - \Phi_j)] + (1 - 1/m_j)(1 - \Phi_j) + \chi_j(1 - \Phi_j)^2 \tag{28}$$

where Φ_j is the volume fraction of a volatile component j; χ_j, the Flory interaction parameter; and m_j, the ratio of molar volumes of polymer and solvent (volatiles). Since the mol fractions of volatile species in the liquid phase are very small under high reaction temperature and vacuum conditions (i.e., $\Phi_j \ll 1$), eq. (28) is reduced to

$$\gamma_j = (1/m_j)\exp(1 - 1/m_j + \chi_j) \tag{29}$$

Little has been reported on the polymer–solvent interaction parameter for the polycarbonate system. Thus, χ_j is estimated by using the following equation[15]:

$$\chi_j = 0.34 + \frac{\hat{v}_j}{RT}(\delta_j - \delta_{\text{poly}})^2 \tag{30}$$

where δ_j and δ_{poly} are the solubility parameters of solvents (phenol and DPC) and bisphenol-A polycarbonate, respectively.[16] The following solubility parameters were used in eq. (30)[14]: δ (phenol) = 12.05 $\text{cal}^{1/2}/\text{cm}^{3/2}$, δ (DPC) = 10.45 $\text{cal}^{1/2}/\text{cm}^{3/2}$ and δ (polycarbonate) = 9.94 $\text{cal}^{1/2}/\text{cm}^{3/2}$. $\hat{v}_j$ is the liquid molar volume (8.787×10^{-2} L/mol for phenol and 1.684×10^{-1} L/mol for DPC). The computed values of χ_j at 250°C are 0.73 for phenol and 0.39 for DPC.

For the calculation of liquid- and vapor-phase compositions and the amount of volatiles removed from the reactor at the beginning of semibatch operation, the following method is used. We assume that as the reactor pressure is reduced, a phase equilibrium is quickly established and the residual amounts of phenol and DPC are removed from the liquid phase. Then, the following component mass balance equations are solved to calculate equilibrium vapor- and liquid-phase compositions:

$$V_g + n_t(x_P\hat{v}_P + x_{B_0}\hat{v}_{B_0} + x_{A_0}\hat{v}_{A_0} + x_{\text{poly}}\hat{v}_{\text{poly}}) = V_t \quad (31)$$

$$x_P + x_{B_0} + x_{A_0} + x_{\text{poly}} = 1 \quad (32)$$

$$\gamma_P p_P^0 x_P + \gamma_{B_0} p_{B_0}^0 x_{B_0} = p_t \quad (33)$$

$$n_t x_p + \frac{\gamma_P p_P^0 x_P V_g}{RT} + P^C = (P)_0 \quad (34)$$

$$n_t x_{B_0} + \frac{\gamma_{B_0} p_{B_0}^0 x_{B_0} V_g}{RT} + B_0^C = (B_0)_0 \quad (35)$$

$$n_t x_{A_0} = (A_0)_0 \quad (36)$$

$$n_t x_{\text{poly}} = (n_{\text{poly}})_0 \quad (37)$$

The symbols in the above expressions are defined in the Notation. In the above, the unknowns are x_P, x_{B_0}, x_{A_0}, x_{poly}, n_t, P^C, and B_0^C. The vapor-phase volume (V_g) is not known exactly because it includes not only the reactor head space but also some vapor space in the distillation column.

The total number of moles in the liquid phase is given as

$$n_t = \frac{f_A - f_B - f_C V_g}{f_D} \quad (38)$$

where

$$f_A = p_{B_0}^0 \gamma_{B_0}(p_P^0 \gamma_P - p_{B_0}^0 \gamma_{B_0}) \times [V_t - \hat{v}_{A_0}(A_0)_0 - \hat{v}_{\text{poly}}(n_{\text{poly}})_0]$$

$$f_B = p_{B_0}^0 \gamma_{B_0}[(A_0)_0 + (n_{\text{poly}})_0](\hat{v}_P p_{B_0}^0 \gamma_{B_0} - \hat{v}_{B_0} p_P^0 \gamma_P)$$

$$f_C = p_{B_0}^0 \gamma_{B_0}(p_P^0 \gamma_P - p_{B_0}^0 \gamma_{B_0})$$

$$f_D = \hat{v}_P(p_t - p_{B_0}^0 \gamma_{B_0}) + \hat{v}_{B_0} p_{B_0}^0 \gamma_{B_0}(p_P^0 \gamma_P - p_t)$$

Since $n_t \le (n_t)_0$ and $B_0 \le (B_0)_0$, where $(n_t)_0$ and $(B_0)_0$ are the initial total number of moles in the liquid phase and the initial number of moles of DPC, respectively, the following condition holds:

$$V_g \ge \frac{f_A - f_B - f_D(n_t)_0}{f_C} \quad (39)$$

The above inequality criterion gives the minimum value of V_g. Using this value, one can solve eqs. (31)-(37). If the computed value of B_0 (number of moles of DPC in the liquid phase) expressed by

$$B_0 = \frac{f_E - f_F V_g - f_G n_t}{f_H} \quad (40)$$

where $f_E = p_P^0 \gamma_P[V_t - (A_0)_0\hat{v}_{A_0} - (n_{\text{poly}})_0\hat{v}_{\text{poly}}]$, $f_F = p_P^0 \gamma_P$, $f_G = \hat{v}_P p_t$, and $f_H = p_P^0 \gamma_P \hat{v}_{B_0} - p_{B_0}^0 \gamma_{B_0} \hat{v}_P$, is larger than $(B_0)_0$, the V_g value is increased and the mass balance equations are solved again until the condition $B_0 \le (B_0)_0$ is satisfied. With this new liquid-phase composition, the kinetic equations are solved in the next time interval and the corresponding equilibrium composition in each phase is calculated.

During the semibatch operation, some loss of DPC may occur because of an imperfect distillation column operation. Thus, it is necessary to estimate the amount of DPC refluxed back to the reactor. Quite obviously, the efficiency of DPC reflux is dependent on the distillation column design and its operation. We used an empirical reflux efficiency factor (ϕ) that is defined as the molar fraction of evaporated DPC that is refluxed back to the reactor in condensed form. Then, $\phi = 1.0$ represents that there is no loss of DPC from the reactor. In reality, of course, ϕ is less than 1.0. It is also possible that the ϕ value may change during the course of semibatch operation. To calculate liquid- and vapor-phase compositions during the semibatch period, we used a flash calculation method that has been used by many authors for similar reaction systems.[17] Figure 2 shows a schematic of the computational procedure. At time t_k, the liquid-phase composition in the previous time step (t_{k-1}) is used first to solve the kinetic model equations [eqs. (11)-(22)]. Then, the following mass balance equations are solved to obtain new vapor- and liquid-phase compositions:

$$G + E + L = F \quad (41)$$

$$(G + E)y_{B_0} + Lx_{B_0} = Fx_{B_0}^F \quad (42)$$

$$(G + E)y_P + Lx_P = Fx_P^F \quad (43)$$

$$y_{B_0} + y_P = 1 \quad (44)$$

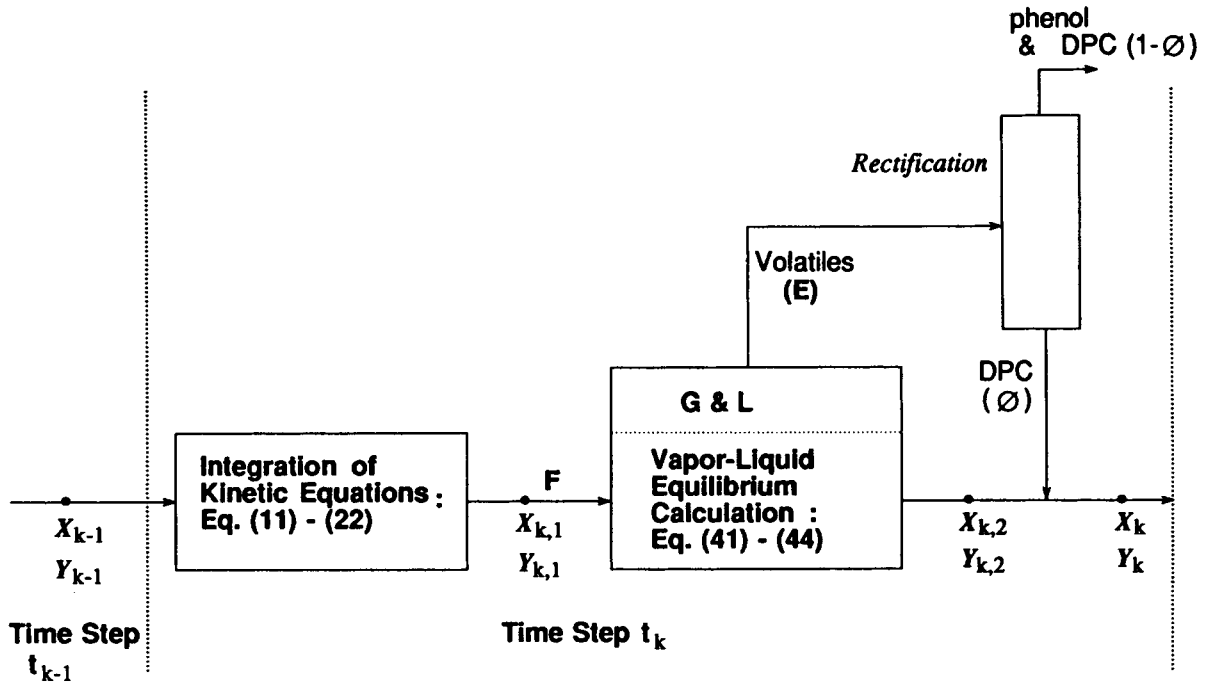

Figure 2 Computational procedure for vapor–liquid composition in semibatch operation.

Here, F represents the number of moles of the feed (in liquid and vapor phases) at t_{k-1} to the flash evaporation process; L, the total number of moles in the liquid phase; G, the total number of moles of volatile species in the vapor phase; and E, the total number of moles of volatile species being removed from the reactor. $x_{B_0}^F$ and x_P^F are the mol fractions of DPC and phenol in the feed (F), respectively. The mol fraction of component j in the liquid phase (x_j) is computed by eqs. (27) and (29). The vapor phase is assumed to follow the ideal gas law. Then, the above equations [eqs. (41)–(44)] are reduced to a single quadratic equation:

$$\alpha y_{B_0}^2 + \beta y_{B_0} - \gamma = 0 \tag{45}$$

where

$$\alpha = \frac{f_c}{f_d} - \frac{f_a}{f_b}$$

$$\beta = \frac{Fx_P^F - f_c}{f_d} + \frac{Fx_{B_0}^F - f_a}{f_b}$$

$$\gamma = \frac{Fx_{B_0}^F}{f_b}$$

$$f_a = \frac{p_t V_g}{RT} + \left(F - \frac{p_t V_g}{RT}\right)\frac{p_t}{p_{B_0}^0 \gamma_{B_0}}$$

$$f_b = 1 - \frac{p_t}{p_{B_0}^0 \gamma_{B_0}}$$

$$f_c = \frac{p_t V_g}{RT} + \left(F - \frac{p_t V_g}{RT}\right)\frac{p_t}{p_P^0 \gamma_P}$$

$$f_d = 1 - \frac{p_t}{p_P^0 \gamma_P}$$

The total number of moles of volatile species being removed from the reactor (E), the total number of moles of volatile species in the vapor phase (G), the total number of moles in the liquid phase (L), the mol fraction of DPC in the liquid phase (x_{B_0}), and the mol fraction of phenol in the liquid phase (x_P) are computed as follows:

$$E = \frac{1}{f_b}\left(\frac{Fx_{B_0}^F}{y_{B_0}} - f_a\right) \tag{46}$$

$$G = \frac{p_t V_g}{RT} \tag{47}$$

$$L = F - E - G \tag{48}$$

$$x_{B_0} = \frac{p_t}{p^0_{B_0}\gamma_{B_0}} y_{B_0} \tag{49}$$

$$x_P = \frac{p_t}{p^0_P\gamma_P} y_P \tag{50}$$

The composition of the vapor phase in the reactor and that of the exit vapor stream are assumed identical. Then, the volume of the reaction mixture at time $t_k(V_k)$ is updated by subtracting the volumes of removed phenol and DPC from the previous liquid-phase volume:

$$V_k = V_{k-1} - Ey_{B_0}(1 - \phi)\hat{v}_{B_0} - Ey_P\hat{v}_P \tag{51}$$

The number of moles of DPC in the liquid phase after reflux is updated as

$$B_0 = Lx_{B_0} + Ey_{B_0}\phi \tag{52}$$

The updated liquid-phase composition is then used for the solution of the model equations [eqs. (11)–(22)] in the next time interval.

RESULTS AND DISCUSSION

As described in the previous section, the polycondensation experiment was carried out in batch and semibatch modes. As the reactor operation was changed from the batch (stage 2) to the semibatch mode (stage 3) by reducing the reactor pressure to 150 mmHg, large amounts of phenol present in the liquid phase ($\sim$ 10 wt % for Run-I and $\sim$ 13 wt % for Run-II) quickly evaporated. At the final moment of the batch reaction, the weight fraction of DPC in the liquid phase was about 12 wt % for Run-I and 10 wt % for Run-II. Since the vapor pressure of DPC at the reaction temperature and pressure was moderate, it is likely that some DPC may have evaporated during the low-pressure semibatch reaction

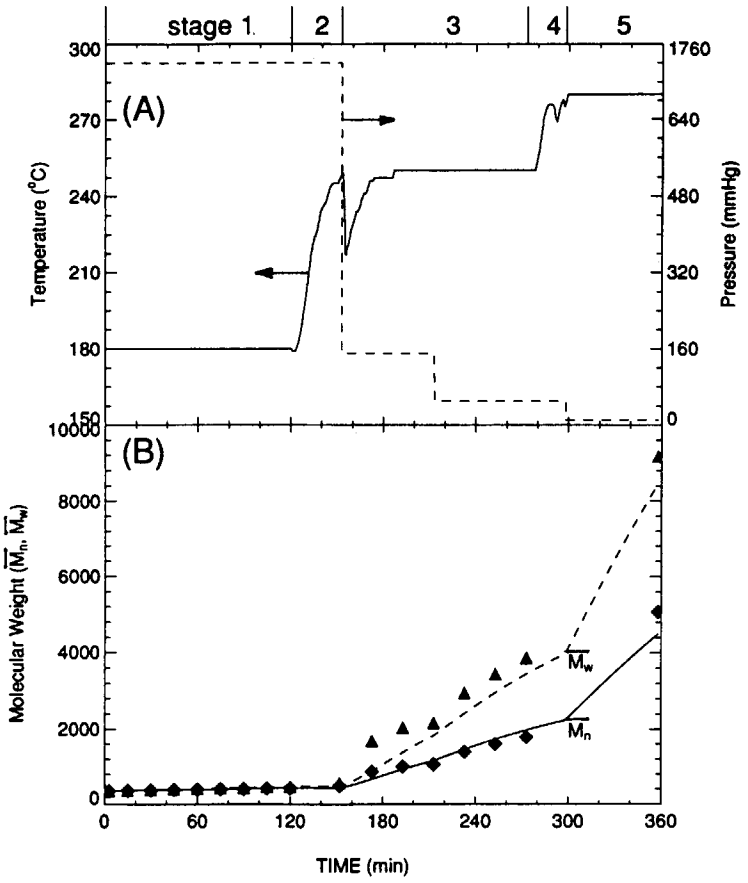

Figure 3 (A) Temperature and pressure variations; (B) polymer molecular weight averages for Run-I ($\phi_3 = \phi_4 = 0.30$, $\phi_5 = 0$).

period. The vaporization and condensation of volatile compounds were clearly observable in stages 3 and 4. However, in the final stage, little condensation was seen in the distillation column.

For the calculation of liquid-phase composition during the semibatch reaction period, the DPC reflux efficiency factor (ϕ) must be known. To estimate the ϕ-factor, one can measure the concentrations of DPC in the liquid phase and in the condensates. However, the amount of DPC present in the liquid phase decreased rapidly as the semibatch reaction (stage 3) started and it was difficult to take condensate samples without disrupting the reactor pressure. It was also observed after the experiment that small amounts of vaporized DPC were deposited on the surface of the reactor inner tops. Thus, measured molecular weight data were used instead to estimate the ϕ-factor values using a standard optimal parameter estimation technique (Rosenbrock's direct search method).[18] It was assumed that in stages 3 and 4 the same ϕ-factor value can be used. In the final stage, where a negligible amount of DPC is present, the ϕ-factor value has no effect on the polymer molecular weight and it has been assumed to be zero (i.e., no reflux of DPC) due to the high reaction temperature and low pressure.

Figure 3(A) shows the temperature and pressure profiles employed in the experimental Run-I. In stage 3, where the reactor pressure was lowered to 150 mmHg, large amounts of volatiles vaporized rapidly, and as a result, the reactor temperature almost immediately decreased to 217°C. In about 34 min, the reactor temperature was brought back to 250°C and maintained at this temperature for 86 min. A further decrease in the pressure during stage 3 caused little variation in the reactor temperature, indicating that a much lesser amount of volatiles was present than in the previous stages. Figure 3(B) shows the polymer molecular weight averages during the experimental period. Here, the symbols are experimental data and the solid lines and the dashed lines represent the model predictions of number-average ($\overline{M_n}$) and weight-average ($\overline{M_w}$) molecular weight of the polymer (excluding DPC, BPA, and phenol), respectively. In solving the reactor model, the actual temperature and pressure profiles shown

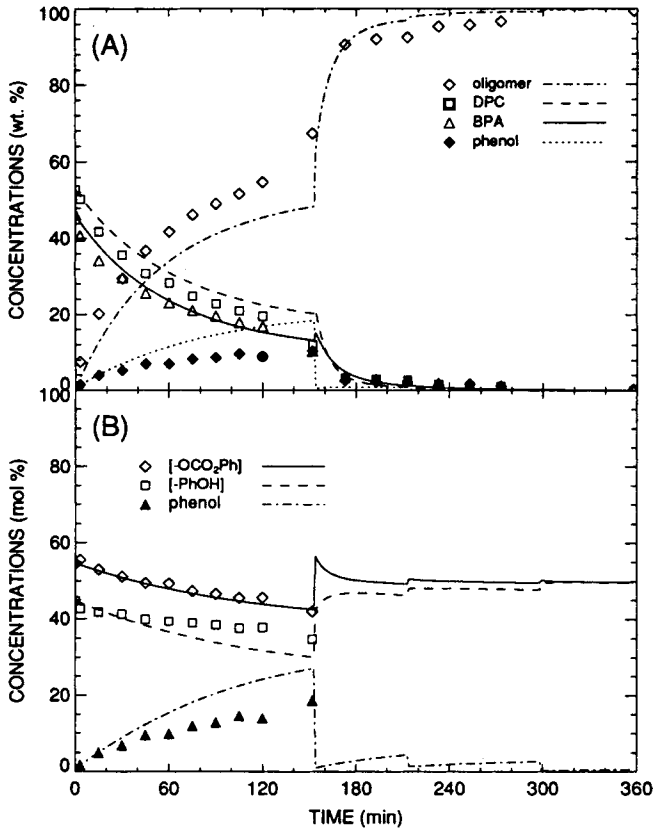

Figure 4 (A) Reaction product compositions; (B) relative concentrations of end groups and phenol for Run-I ($\phi_3 = \phi_4 = 0.30$, $\phi_5 = 0$).

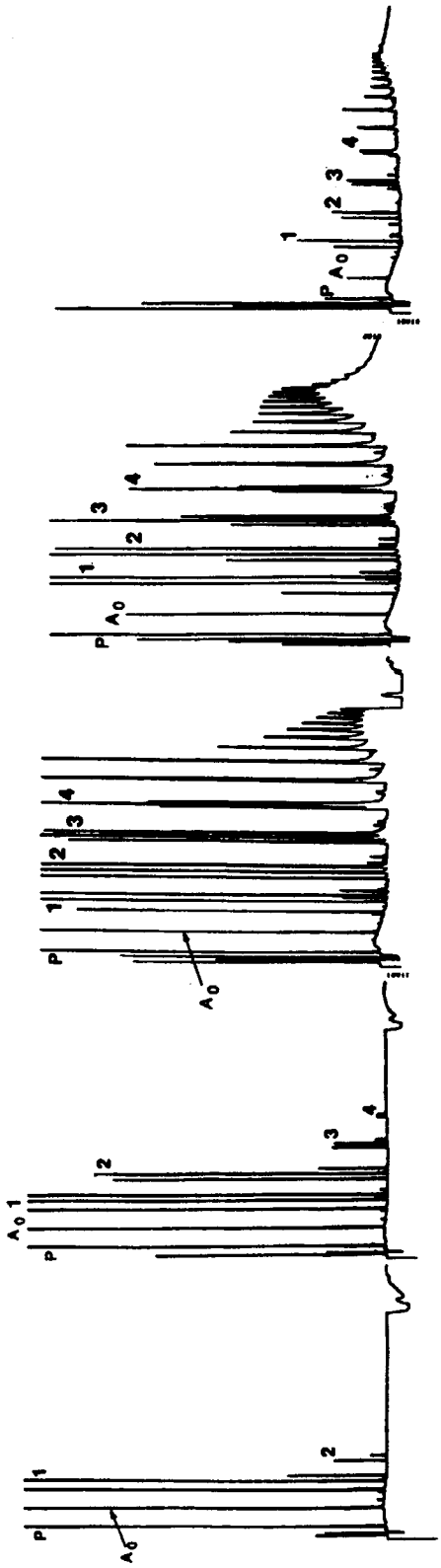

(A) Batch (180 °C) at 15 min

(B) Batch (180 °C) at 120 min

(C) Semibatch (250 °C, 150 mmHg) at 193 min

(D) Semibatch (250 °C, 50 mmHg) at 273 min

(E) Semibatch (280 °C, 10 mmHg) at 358 min

Figure 5 HPLC chromatograms for the reaction samples of Run-I.

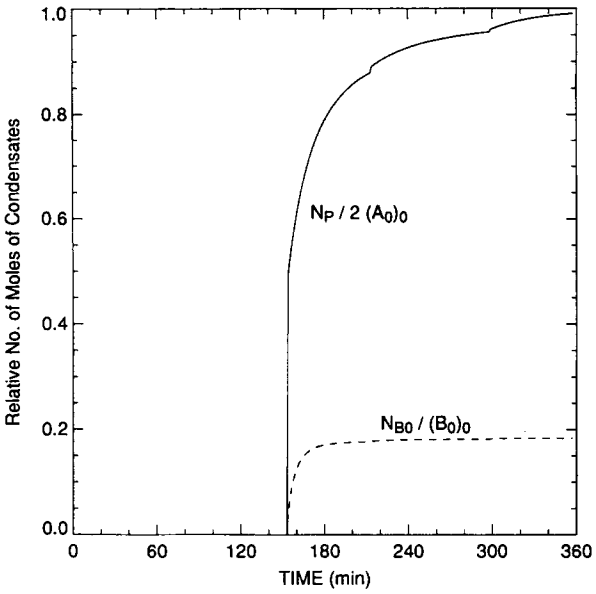

Figure 6 Cumulative number of moles of phenol (N_P) and DPC (N_{B_0}) in condensates for Run-I ($\phi_3 = \phi_4 = 0.30$, $\phi_5 = 0$).

in Figure 3(A) were input to the model. The estimated ϕ-factor value for stages 3 and 4 in this run was 0.30.

Note that the temperature increase in stage 2 (batch reaction) has little effect on the molecular weight; however, as the pressure is lowered to 150 mmHg in stage 3, the molecular weight increases almost linearly with time. In stages 4 and 5, the melt viscosity was so high that it was impossible to take samples from the reactor using the sampling valve. It is seen that the model predictions are in reasonable agreement with the experimental molecular weight data for the duration of the reaction.

Figure 4(A) shows the concentrations (in wt %) of monomers, phenol, and oligomers in the reaction mixture. Although the overall agreement between the model predictions and the experimental data is reasonable, some discrepancies are seen in phenol and oligomer concentrations during the batch reaction (stages 1 and 2). It is thought that such discrepancies are possibly due to the partial loss of phenol when hot samples were withdrawn from the

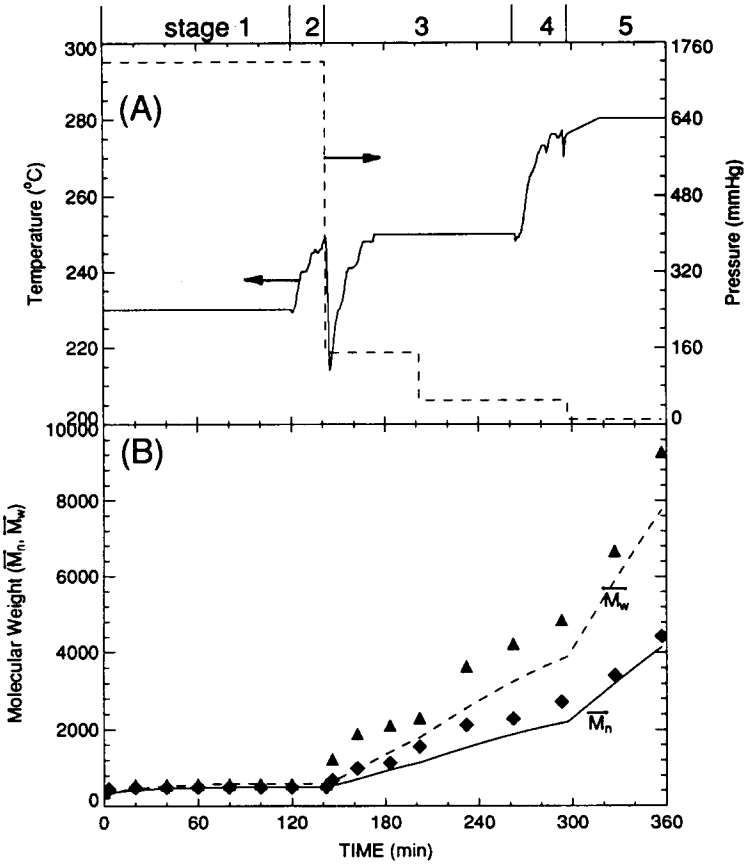

Figure 7 (A) Temperature and pressure variations; (B) polymer molecular weight averages for Run-II ($\phi_3 = \phi_4 = 0.61$, $\phi_5 = 0$).

reactor using a vacuum-assisted sampling flask. Figure 4(A) also shows that the reaction samples withdrawn during the semibatch operations consist mainly of oligomers and the amounts of phenol and DPC in the liquid phase are negligibly small. It is seen that the predicted oligomer concentrations in the semibatch period are in good agreement with the experimental data.

Figure 4(B) shows the relative concentrations (in mol %) of the two end groups and phenol in the reaction mixture. The end-group concentrations were measured by HPLC. During the batch period, the ratio of the phenyl carbonate group to the hydroxyl group decreases only slightly. As the reaction advances to the last stage (higher temperature and lower pressure), the ratio approaches unity. In stages 3, 4, and 5, the oligomers having more than four repeating units were not separated by HPLC. Thus, it was not possible to measure individual end-group concentrations in these stages. Figure 5 shows the original HPLC chromatograms for samples withdrawn at different times. It is seen that the reaction samples taken during the semibatch reaction periods include oligomers with $n \geq 5$ and the corresponding HPLC chromatograms show no separation of each oligomeric species (i.e., A_n, B_n, and C_n).

Figure 6 shows the relative number of moles of phenol and DPC in the condensates [$N_P/2(A_0)_0$ for phenol and $N_{B_0}/(B_0)_0$ for DPC] computed by the model. At 100% conversion, the theoretical amount of phenol liberated should be twice the initial moles of BPA charged in the reactor. It is seen that the condensates contain about 18 mol % DPC (based on the initial amount of DPC) after the end of the reaction. It also shows that the loss of DPC occurs mostly at the beginning of the semibatch operation. These figures indicate that the condensate is a mixture of phenol and DPC and, thus, the extent of reaction in the semibatch reaction is not directly measurable from the total amount of volatiles removed from the reactor unless the condensate composition is monitored continuously.

The temperature and pressure profiles employed in another multistage polymerization experiment (Run-II) are shown in Figure 7(A). The major dif-

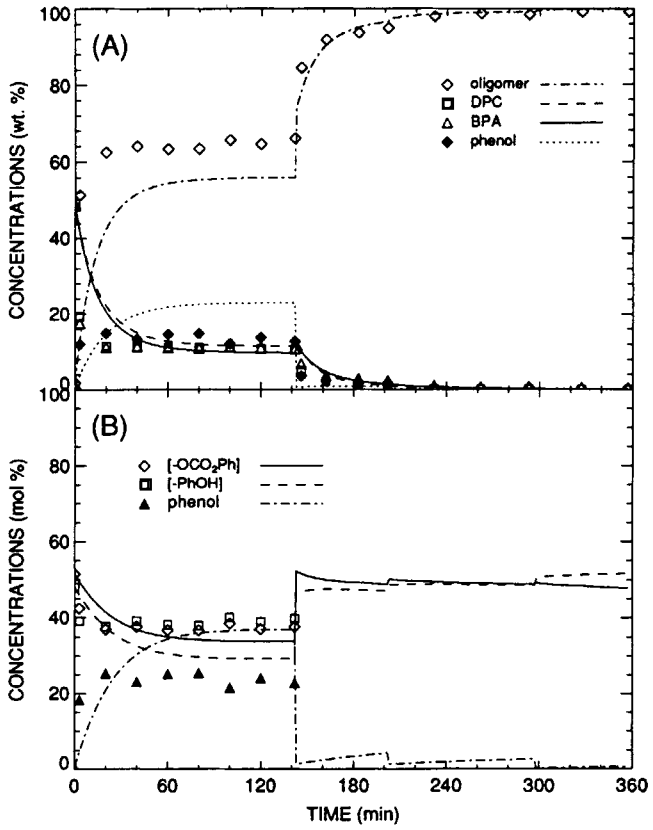

Figure 8 (A) Reaction product compositions; (B) relative concentrations of end groups and phenol for Run-II ($\phi_3 = \phi_4 = 0.61$, $\phi_5 = 0$).

ferences between Run-II and Run-I are the final batch reaction temperature and the initial DPC/BPA mol ratio. As the reactor pressure was lowered to 150 mmHg (stage 3), the reaction temperature quickly dropped to 214°C. The reactor temperature was brought back to 250°C in about 31 min. Figure 7(B) shows the measured and predicted polymer molecular weight averages ($\overline{M_n}$ and $\overline{M_w}$). Despite the differences in the reaction temperature and the DPC/BPA mol ratio, the molecular weight in stages 1 and 2 for Run-II is almost identical to that for Run-I. The ϕ-factor value used in the simulation was 0.61 for stages 3 and 4. Although the predicted $\overline{M_n}$ values are in good agreement with the experimental data, predicted $\overline{M_w}$ values are lower than the experimental data. Although the molecular weights at the beginning of semibatch operations were almost identical in both cases, it is seen that the oligomer molecular weights for Run-II are higher than that for Run-I.

The composition of the reaction mixture (in wt %) and the relative concentrations of end groups and phenol in the reaction mixture (in mol %) are shown in Figure 8, which is qualitatively similar to Figure 4. Figure 8(B) shows that the ratio of the phenyl carbonate group to the hydroxyl group is close to unity in batch and semibatch periods. Therefore, the higher molecular weight observed in Run-II can be attributed to an improved stoichiometric balance of the functional end groups. Since it was not possible to withdraw the condensate sample from the receiver during the semibatch operation, the condensate recovered after the experiment was analyzed by HPLC. It was found that a negligible amount of DPC was present in the condensate. However, a thin layer of solidified DPC was found at the surface of reactor inner tops after the experiment.

Recall that the ϕ-factor was estimated from the measured $\overline{M_n}$ data. In fact, the amount of lost DPC may be dependent on the design and operation of a distillation column and thus we examined the sensitivity of the model simulations to ϕ values. Figure 9 shows the effect of ϕ-factor values (ϕ_3 and ϕ_4) on

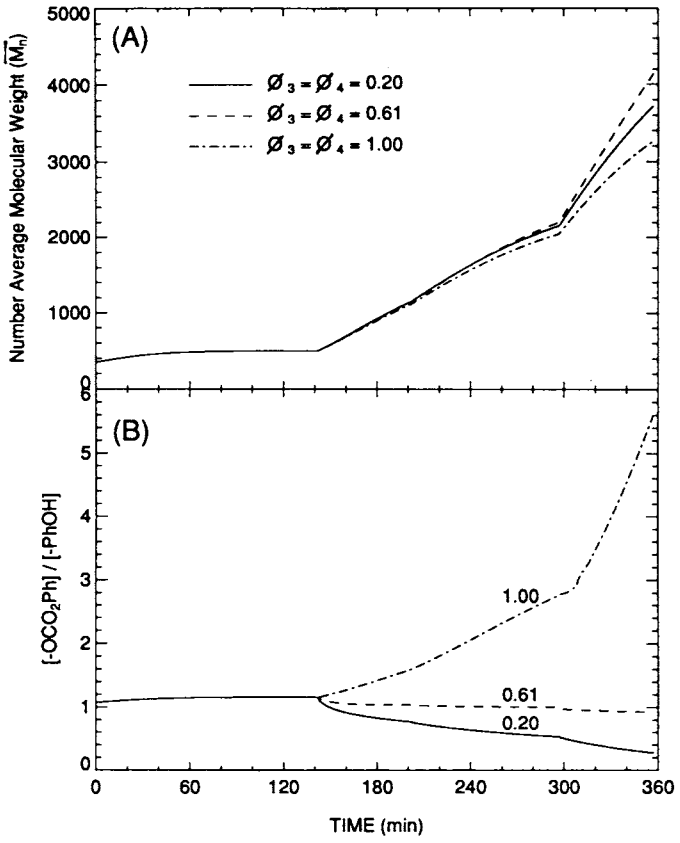

Figure 9 (A) Effect of DPC reflux ratio on polymer molecular weight ($\bar{M}_n$) and (B) the effect of mol ratio of two end groups (based on Run-II; $\phi_5 = 0.0$).

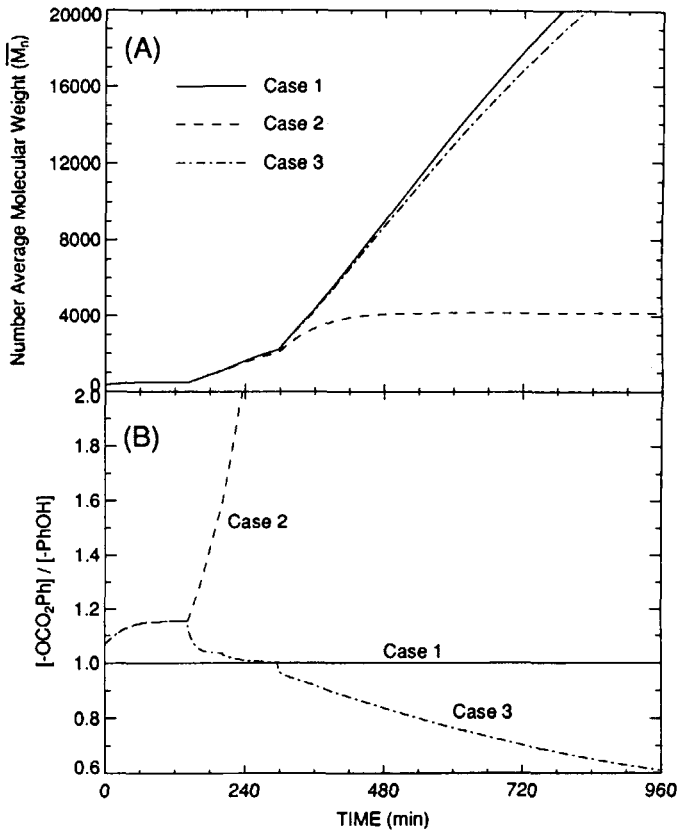

Figure 10 Effect of DPC reflux ratio in continued semibatch reaction process: (A) polymer molecular weight ($\bar{M}_n$); (B) mol ratio of two end groups (based on Run-II) [Case 1, $(DPC/BPA)_0 = 1.0$, no loss of DPC; Case 2, $(DPC/BPA)_0 = 1.07$, no loss of DPC; Case 3, $(DPC/BPA)_0 = 1.07$, $\phi_3 = \phi_4 = 0.61$, $\phi_5 = \phi_6 = 0$]; $0 \leq t \leq 142$ min, batch reaction; $143 \leq t \leq 957$ min, semibatch reaction.

the polymer molecular weight ($\overline{M_n}$) and the mol fraction of phenyl carbonate group in the liquid phase calculated with experimental conditions for Run-II. If no loss of DPC is assumed (i.e., $\phi = 1.0$), there is always an excess amount of the phenyl carbonate group in the liquid phase because the initial monomer mixture contains 7% excess DPC. Thus, at the end of the semibatch operation (stage 5), the reaction mixture will contain a large excess of the phenyl carbonate group. However, for $\phi = 0.61$, a partial loss of DPC during the semibatch operation makes the molar ratio of the phenyl carbonate group to the hydroxyl group close to unity. As a result, the polymer molecular weight is higher than that in the case for $\phi = 1.0$. If the ϕ-factor value is far smaller than 0.61 (e.g., $\phi = 0.20$), a significant amount of DPC is lost, leading to an excess of the hydroxyl group and decreased molecular weight. Since the conversions of end groups do not increase very much in stages 3 and 4, the molecular weight is little affected by the ϕ-values.

To further investigate the effect of the ϕ-factor on the polymer molecular weight in the later stage of the semibatch reaction, the model simulations were carried out as follows: It was assumed that Run-II was continued after stage 5 by operating the reactor at 280°C and 0.5 mmHg for 2 h (stage 6). Figure 10 shows the results for three cases: Case 1, $(DPC/BPA)_0 = 1.0$, no loss of DPC; Case 2, $(DPC/BPA)_0 = 1.07$, no loss of DPC; and Case 3, $(DPC/BPA)_0 = 1.07$, $\phi_3 = \phi_4 = 0.61$, and $\phi_5 = \phi_6 = 0.0$. From these model simulations, it becomes clear that maintaining the equimolar ratio of end groups is important to obtain high molecular weight polymers.

CONCLUDING REMARKS

In this paper, a multistage melt transesterification process has been investigated for the synthesis of bisphenol-A polycarbonate prepolymers through experimental and reactor modeling studies. The re-

action products for both batch and semibatch periods were analyzed by HPLC to determine the conversion of reactive end groups and the composition of the reaction mixture. A molecular species model was proposed and solved for the two experimental conditions and the overall agreement between the model predictions and experimental data was reasonable. In operating the experimental reactor, clogging of monomer feed lines and the vacuumed product withdrawal lines was frequently encountered when heating was not applied properly. In our experiment, a partial loss of DPC monomer occurred and we introduced an empirical reflux efficiency factor to account for the loss of DPC from the reaction mixture. It was observed that maintaining the proper ratio of reactive end groups becomes important in the later stages of the semibatch process. However, a practical difficulty in quantifying the loss of DPC lies in that the efficiency of the DPC reflux is dependent on the design and operation of a distillation column, heating, and insulation of the reactor equipment. Our experimental results indicate that the use of a slight excess of DPC will be useful to compensate for the loss of DPC during the low-pressure polycondensation process.

This research was supported by the National Science Foundation (CBT-85-52428) and in part by Dow Chemical Company (Midland, MI) for which we express our sincere gratitude. We would also like thank Dr. Thomas Chamberlin for his assistance in analyzing the reaction samples.

NOTATION

B_0^C	number of moles of DPC (B_0) removed from the reactor [mol]
$[C^*]$	catalyst concentration [mol/L]
$(j)_0$	number of moles of j before the start of semibatch operation [mol]
k	effective forward reaction rate constant [L/mol min]
k'	effective reverse reaction rate constant [L/mol min]
$\boldsymbol{k}$	forward transesterification rate constant in the catalyzed reaction [L^2/mol^2 min]
$\boldsymbol{k}'$	reverse transesterification rate constant in the catalyzed reaction [L^2/mol^2 min]
m_j	ratio of molar volumes of polymer and solvent j
n_t	total number of moles in the liquid phase [mol]
n_{poly}	total number of moles of polymeric species ($= \lambda_{A,0} + \lambda_{B,0} + \lambda_{C,0}$) [mol]
N^*	number of moles of catalyst added [mol]
N_P	cumulative number of moles of phenol in condensates [mol]
N_{B_0}	cumulative number of moles of DPC in condensates [mol]
P	number of moles of phenol in the liquid phase [mol]
P^C	number of moles of phenol (P) removed from the reactor [mol]
p_j	partial pressure of component j [mmHg]
p_t	total reactor pressure [mmHg]
p_j^0	saturated vapor pressure of component j [mmHg]
V	reaction volume [L]
V_t	total reactor volume including liquid and vapor phases [L]
V_g	vapor-phase volume [L]
$\hat{v}_j$	molar volume of component j in the liquid phase [L/mol]
x_j	liquid-phase mole fraction of component j
y_j	vapor-phase mole fraction of component j
γ_j	activity coefficient of component j
ϕ	reflux efficiency factor for DPC
Φ_j	volume fraction of component j
χ_j	Flory interaction parameter of component j
δ_j	solubility parameter of component j [$cal^{1/2}/cm^{3/2}$]
δ_{poly}	solubility parameter of bisphenol-A polycarbonate [$cal^{1/2}/cm^{3/2}$]
BPA	bisphenol-A (4,4-dihydroxydiphenyl 2,2-propane)
DPC	diphenyl carbonate
HPLC	high-performance liquid chromatography

Subscripts

A_0	bisphenol-A
B_0	diphenyl carbonate
P	phenol

REFERENCES

1. I. P. Losev, O. V. Smirnova, and Ye. V. Smurova, *Polym. Sci. USSR,* **5**(1), 662–670 (1963).
2. Y. Kim, PhD Thesis, University of Maryland, College Park, MD, 1992.
3. E. Turska and A. M. Wróbel, *Polymer,* **11,** 409–414 (1970).
4. E. Turska and A. M. Wróbel, *Polymer,* **11,** 415–420 (1970).
5. S. N. Hersh and K. Y. Choi, *J. Appl. Polym. Sci.,* **41,** 1033–1046 (1990).
6. Y. Kim, K. Y. Choi, and T. A. Chamberlin, *I & EC Res.,* to appear.

7. D. J. Brunelle, U.S. Pat. 4,321,356 (1982) (assigned to General Electric Co.).
8. Ch. Bailly, D. Daoust, R. Legras, J. P. Mercier, and M. de Valck, *Polymer,* **27,** 776–782 (1986).
9. K. Tai, Y. Arai, H. Teranishi, and T. Tagawa, *J. Appl. Polym. Sci.,* **25,** 1789–1792 (1980).
10. K. N. Marsh, Ed., *TRC Thermodynamic Tables: Non-Hydrocarbons,* Thermodynamics Research Center, The Texas A & M University System, College Station, TX, 1985, Vol. 5, p. K-6400, Table 23-2-1-(33.1000)-k.
11. B. D. Smith and R. Srivastava, *Thermodynamic Data for Pure Compounds,* Pt. B, Elsevier Sci. Publishing, Amsterdam, The Netherlands (1986).
12. J. Buckingham, Ed., *Dictionary of Organic Compounds,* 5th ed., Chapman & Hill, New York, 1982.
13. G. Smith, J. Winnick, D. S. Abrams, and J. M. Prausnitz, *Can. J. Chem. Eng.,* **54,** 337–343 (1976).
14. J. M. Prausnitz, *Molecular Thermodynamics of Fluid-Phase Equilibria,* Prentice-Hall, Englewood Cliffs, NJ, 1969.
15. K. Ravindranath and R. A. Mashelkar, *Chem. Eng. Sci.,* **41**(9), 2197–2224 (1986).
16. D. W. Van Krevelen and P. J. Hoftyzer, *Properties of Polymers,* Elsevier, Amsterdam, The Netherlands, 1976.
17. K. Ravindranath and R. A. Mashelkar, *J. Appl. Polym. Sci.,* **26,** 3179–3204 (1981).
18. H. H. Rosenbrock, *Comput. J.,* **3,** 175–184 (1960).

Received August 13, 1992
Accepted October 28, 1992